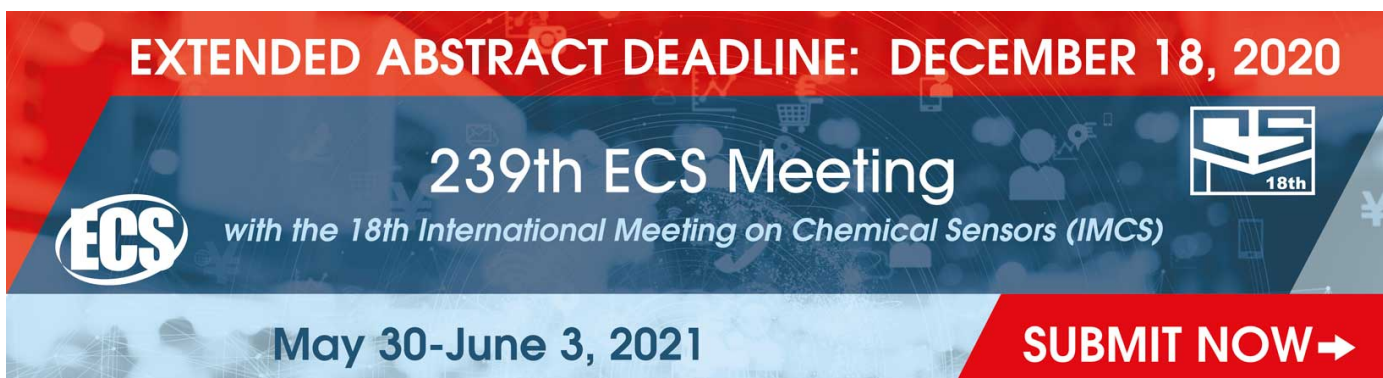


PAPER • OPEN ACCESS

Grain Growth Prediction of Bead-on-Plate with Filler Wire SS316L using FEM

To cite this article: Muhd Faiz Mat *et al* 2020 *IOP Conf. Ser.: Mater. Sci. Eng.* **834** 012009

View the [article online](#) for updates and enhancements.



EXTENDED ABSTRACT DEADLINE: DECEMBER 18, 2020

239th ECS Meeting
with the 18th International Meeting on Chemical Sensors (IMCS)

May 30-June 3, 2021

SUBMIT NOW →

The banner features a red top section with white text, a blue middle section with white text and logos, and a red bottom section with white text. The ECS logo is on the left, and the IMCS 18th logo is on the right. The background of the blue section shows a network of nodes and lines.

Grain Growth Prediction of Bead-on-Plate with Filler Wire SS316L using FEM

Muhd Faiz Mat¹, Yupiter H. P. Manurung*¹, Norasiah Muhammad², Anton Dittler³, Mohd Syakir Abd Ghani¹, Martin Leitner⁴

¹Faculty of Mechanical Engineering, Universiti Teknologi MARA (UiTM), Malaysia.

²Mechanical Engineering Department, Politeknik Sultan Salahuddin Abdul Aziz Shah, Malaysia.

³Hochschule Osnabrück, Osnabrück, Germany.

⁴Chair of Mechanical Engineering, Montanuniversität Leoben, Austria.

*yupiter.manurung@uitm.edu.my

Abstract. This fundamental investigation presents the study on the grain growth prediction for bead-on-plate of stainless steel SS316L. At first, the numerical model is developed by using basic equation with ordinary differential equation for calculating the grain growth with the presence of growing precipitates. The modified kinetic constant (M_o^*) is defined based on experimental investigation using quench and deformation dilatometer for peak temperature of 1200°C and holding time of 30 seconds. The FEM simulation is conducted based on temperature dependant materials properties using MSC Marc/Mentat. As the outcome various temperature ranges for calculating the grain growth are presented. These results are to be used for further investigation using experimental bead-on-plate.

1. Introduction

The microstructure and mechanical properties of the heat-affected zone (HAZ) of welded metal is significantly affected by the continuous welding heat input. This will affect the grain structure that affects the strength, toughness, ductility and corrosion resistance of the alloys [1]. The high operating temperature leads to change of grain size. Therefore, the attempt to predict the grain size is crucial to evaluate the effect of grain growth to degree of sensitization (DOS) as the inverse co-relationship of grain size and DOS was conclude in [2]. The modelling of the microstructural changes within the welded parts are the utmost important for engineers. It should be noted that certain software, based on thermal and metallurgical modelling have been developed to predict the grain size at HAZ's in multipass welding and their effects on mechanical properties. The objective is to predict the component properties and if applicable used the numerical simulation for other potential application. Thus, it is important that the temperature-dependant material behaviour is known.

Due to its good weldability, corrosion resistance and adequate high temperature mechanical properties, austenitic stainless steel (ASS) is used in different industries, such as petrochemical, shipbuilding, and nuclear industries. These steels are non-magnetic, stable at room temperature, and cannot be hardened by heat treatment [3–5]. In recent years, significant contributions have been made to predict the grain behaviour of surface treated component rather than welded components using simulation software. As a preliminary investigation towards grain behaviour of welded components using simulation software for welding process, material information is very important as grain behaviour is highly dependent on the material chemical composition. Different technique and models have been employed to simulate arc welding process with various physical phenomena was observed and predicted.



H. Jamshidi have investigate the grain growth kinetics of SS304 to predict the grain size [6]. Investigation of grain size after Gas Metal Arc Welding on dissimilar material SS304 and SS316 (filler) has proven that alloy segregation and prolong cooling time also generate coarse austenite grain structures next to the sensitized region at the fusion zone, and it became weaker than the surrounding structure [7]. Thus, the prediction of the grain size will focus at the HAZ zone as it is the area adjacent to the weld that was heated high enough to affect its microstructure but not enough to melt it. By undergoing microstructural changes, the HAZ has different mechanical and physical properties than the weld and the adjacent base metal [8].

In this study, an attempt has been made to estimate the grain size in the HAZ of filler wire SS316L using bead-on-plate process. In industries like aeronautical, aerospace, chemical, petrochemical, and marine one of the most important materials are the nickel-based alloys. High corrosion resistance, high strength at both ambient and elevated temperatures, and good ductility and toughness at low temperatures are among the main mechanical properties of the nickel-based alloys [9]. Grain size of SS316L has been experimentally determined to obtain the preliminary modified kinetic constant (M_0^*) of the said material. Then, a subroutine for MSC Marc/Mentat grain size calculation have been developed based on the average grain size in the presence of growing precipitates.

2. Numerical Computational and FEM Simulation

2.1 Numerical Computation for Grain Growth prediction.

The grain size behaviour of type 304 stainless steel in low cycle fatigue at elevated temperature was investigated by Yada based on the smooth specimens with various grain sizes [10]. As default the grain size calculation within MSC Marc/Mentat are based on Yada's model is more suitable for forming process. However, the capability to use a different analytical modelling of grain growth is available by developing a subroutine integrated within MSC Marc/Mentat software. As such, there is a need to implement a new mathematical model to simulate this phenomenon. The mathematical model for grain growth has been selected from [11]. This preliminary investigation focuses on grain growth in the presence of growing precipitates. Since the HAZ is heated to temperature approaching the solidus temperature of the alloy, many precipitates that are present in the base metal may dissolve. Carbides and nitrides are the most likely precipitate form in the HAZ of austenitic stainless steel [12].

General equation for grain growth.

$$\frac{\partial g}{\partial t} = M_0^* \exp \left[-\frac{Q_{app}}{RT(t)} \right] \left[\frac{1}{g} - \frac{1}{g_{lim}} \right]^{\left(\frac{1}{n}-1\right)} \quad (1)$$

Where;

M_0^* = Modified kinetic constant ($\mu m^2 s^{-1}$)

Q_{app} = Activation energy ($kJ mol^{-1}$)

R = Gas constant ($8314 J K^{-1} mol^{-1}$)

T = Absolute temperature (K)

\underline{g} = Average/initial grain size (μm)

The \underline{g}_{lim} value depends on the different cases.

The grain growth in the presence of growing precipitates,

Where;

$$\underline{g}_{lim} = \left[\left(\underline{g}_{lim}^0 \right) + \left(\frac{k}{f_0} \right)^3 I_2 \right]^{\frac{1}{3}}$$

$$\underline{g}_{lim}^0 = k \frac{r_0}{f_0}$$

$$I_2 = C_5 \int_0^t \frac{1}{T(t)} \exp \left[-\frac{Q_s}{RT(t)} \right] dt \quad (2)$$

r_0 = Initial radius of precipitate (μm)

f_0 = Initial volume fraction of precipitate

I_2 = Kinetic strength of the thermal cycle particle coarsening (μm^3)

C_5 = Kinetic constant

Q_s = Activation energy for coarsening process (kJ mol^{-1})

The implementation of the mathematical model is established by writing a user subroutine to be used by the finite element analysis (FEA) software. The newly developed grain growth model based on the models of Zener, Hellman and Hillbert and Gladman estimate the limiting austenite grain size D_{lim} in the transformed parts of the weld HAZ when the oxygen and sulphur contents of the as-deposited weld metal are 0.04 and 0.01 wt%, respectively [11]. The grain growth model was suitable to be used as the material selected was the same category as type 316 austenitic stainless steel. The data used was compiled from miscellaneous source and experiment shown in Table 1.

Table 1. Data used for type 316 austenitic stainless steel

| n | Q_{app} (kJ mol^{-1}) | ΔH^* (kJ mol^{-1}) | Q_d (kJ mol^{-1}) | D_{lim}° (μm) | D° (μm) | M_o^* ($\mu\text{m}^2 \text{s}^{-1}$) | Ω^* ($\mu\text{m}^2 \text{s}^{-1}$) |
|------------------|---------------------------------------|--|-----------------------------------|---|----------------------------------|--|---|
| 0.5 ^b | 224 ^b | 60 ^b | 240 ^b | 18 ^a | 18 ^a | 2000×10^9 ^a | 2.1×10^{14} ^b |

^a Value obtained from experiment for preliminary Modified kinetic constant (M_o)

^b Value obtained from miscellaneous sources

To find the parameters of grain size for 316 stainless steels, an experiment has been conducted. The chemical composition is given in Table 2. Subsequent experiment is needed to identify and verify the data used based on the raw material used for the investigation. Firstly, the specimens as shown in Figure 2 had been through heat treatment process using DIL 805A/D quenching and deformations dilatometers. This regulated experiment controls the exposed temperatures for the heat treatment process were 1200 °C (peak temperature) with a holding time of 30 s. Afterwards an epoxy mount has been used for the specimens. After 12 hours, the specimens were grinded by forcipol grinding machine. The specimens were polished for better surface texture. Then a metallographic observation was conducted, the specimens were etched with V2A solution for 10 minutes and consequently the grain size of the 316 stainless steel specimens were defined.



Figure 1. DIL 805A/D Dilatometer



Figure 2. SS316L specimens

2.2 FEM Simulation for Grain Growth prediction on bead-on-plate using MSC Marc/Mentat

The thermo-mechanical simulation of the welding process is applied using MSC MSC Marc/Mentat. The simulation is divided into 3 stages; preprocessing, solving and post-processing. The general flow of the simulation is displayed in Figure 3 below, where the first seven stages are preprocessing followed by solving and post processing. The chosen type of meshing is quad-mesh due to the geometric shape of the work piece to be relatively simplified. Since not much strain and change of shape is expected, using simplified mesh is done to save computing time and ease the modelling effort.

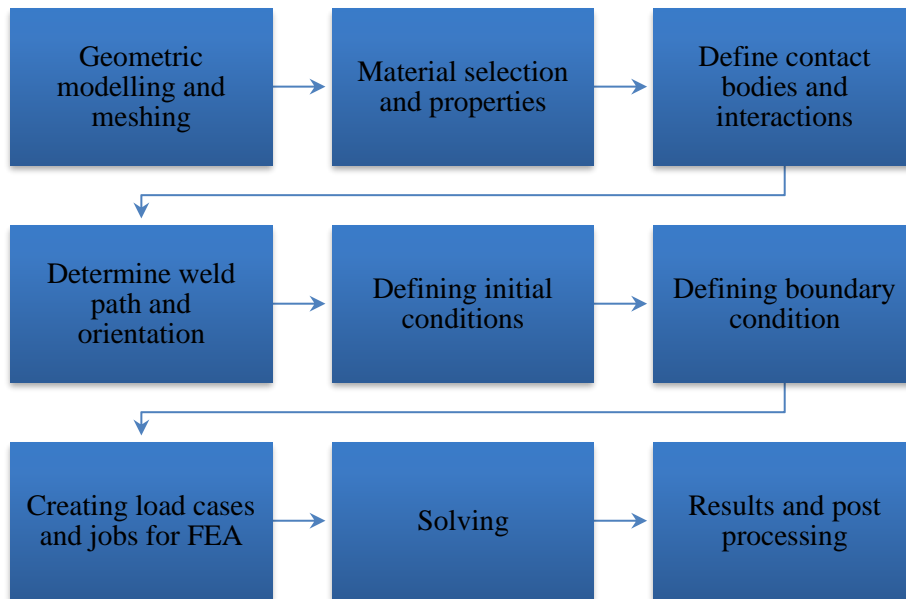


Figure 3. General Flowchart of simulation procedure using MSC Marc/Mentat [10]

2.2.1 Geometrical Modelling

A schematic illustration of Finite Element (FE) models of bead on plate is displayed in Figure 4. To build the model as accurate as possible the entire FE model of bead on plate components consists of a Table (rigid solid), the substrate material (60 mm x 140 mm x 4 mm) and weld beads was developed. A rectangular-shape model of 90 mm of length along with 6 mm in width was modelled as weld filler. Simulating the experiment, the welding trajectory is located at the upper layer of the base plate. The location and forces of the clamping conditions is important to be as identical to the experiment also has been included in the simulation. This is important as clamping conditions such as clamping location, clamping forces and clamping connection has been previously studied will affect the distortion value of WAAM process [14–17]. Finer elements also have been considered along the welding HAZ for research purposes.

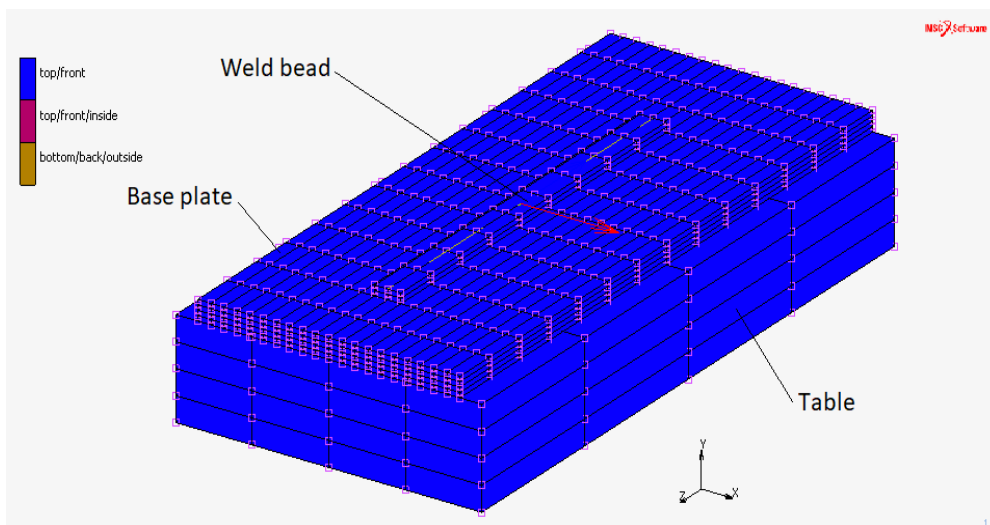


Figure 4. FEM Geometrical modelling

2.2.2 Material characterisation and modelling

SS316L Stainless Steel has been used as the filler material, and the base plate material to predict the grain size. This type of stainless steel has been widely used in many applications, combining good strength with good welding properties. It is nonmagnetic in the annealed condition but can become slightly magnetic because of cold working or welding [18]. Table 2 shows the chemical composition based on international standard and the experimental results obtained using EDX with scanning electron microscope (SEM). In this simulation both thermo-physical and thermo-mechanical material properties should be imported into FEM simulation using existing database from the software library, but as SS316L material wasn't in the default database, it has been added manually by referring to Simufact additive software. The thermo-physical and thermo-mechanical properties are as presented in Figure 5, 6, 7 and 8.

Table 2. SS316L chemical composition

| Catalog | SS316L Filler Wire | | | | | | |
|----------------|---------------------------|------|------|------|------|------|------|
| SiK | 0.9 | 0.4 | 0.7 | 0.9 | 0.7 | 0.8 | 0.8 |
| Average | 0.7 | | | | | | |
| MoL | 2.6 | 0.7 | 1.3 | 1.4 | 1.3 | 1.4 | 1.1 |
| Average | 1.2 | | | | | | |
| CrK | 18.4 | 18.4 | 17.9 | 17.6 | 17.4 | 17.7 | 17.4 |
| Average | 17.7 | | | | | | |
| MnK | 1.8 | 2.6 | 2.5 | 2.6 | 2.3 | 2.1 | 2.5 |
| Average | 2.40 | | | | | | |
| FeK | Balance | 65.5 | 66.7 | 67 | 67.6 | 66.5 | 67.5 |
| Average | 66.8 | | | | | | |
| NiK | 12.2 | 12.8 | 11.6 | 12 | 12.2 | 10.6 | 12.3 |
| Average | 11.91 | | | | | | |

The mechanical and physical properties are as presented in Table 3.

Table 3. Mechanical and physical properties of SS316L

| Properties | Values |
|---------------------------------|---------------|
| Yield Strength [MPa] | 25,000 |
| Ultimate Tensile Strength [Mpa] | 70,000 |
| Poisson's ratio [v] | 0.275 |
| Melting Range [°C] | 1390 - 1440 |
| Modulus of Elasticity [GPa] | 200 |

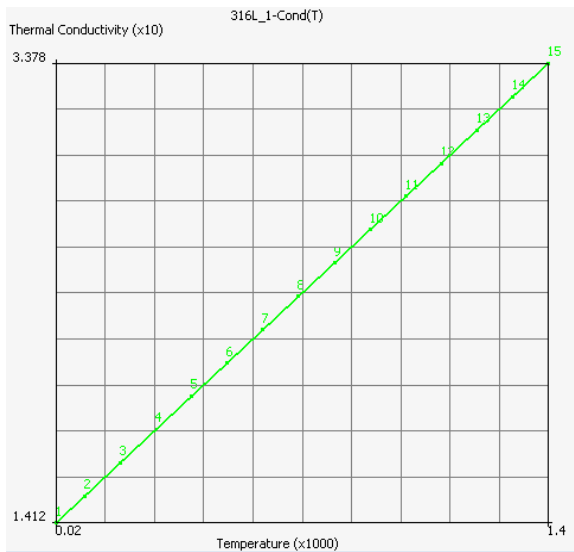


Figure 5. Thermal expansion SS316L

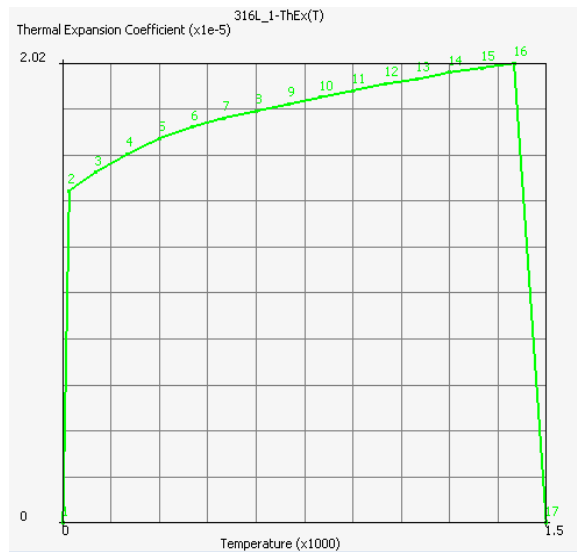


Figure 6. Thermal conductivity SS316L

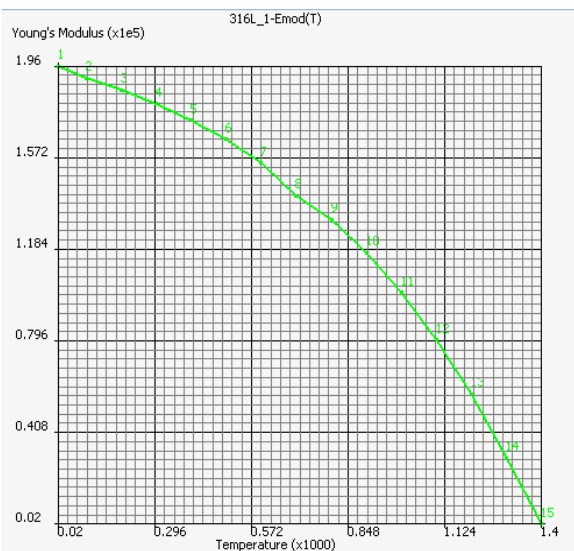


Figure 7. Young's modulus SS316L

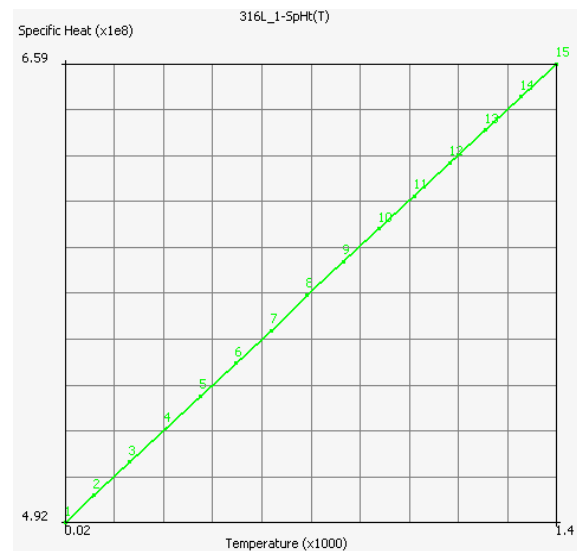


Figure 8. Specific heat SS316L

2.2.3 Welding parameter and heat source model

Table 4 displays the parameters which are implemented on the commercial software MSC Marc/Mentat. Therefore, the Current (I) and the Voltage (V) are considered under the power equation. The assigned travel speed was based on the experimental welding speed to have a more accurate model.

| Welding parameters | Value |
|---------------------------|--------------|
| Current, I (A) | 172 |
| Voltage, V (V) | 20 |
| Travel speed, v (mm/s) | 5.0 |

In a welding simulation using FEM, an important factor to be considered is the heat source model. The Goldak double ellipsoid model is mostly used as the heat source model in a typical simulation of an arc welding process as in Figure 6. This is due to its accuracy and reliability in representing the shape and distribution of the heat flux proposed by Goldak et al [19]. The heat input model is by no mean

constrained to the double ellipsoid. A thorough description of this heat source model can be found in [20]. The schematic of the heat source model is shown in Figure 9. The heat source parameters were obtained from previous studies [21].

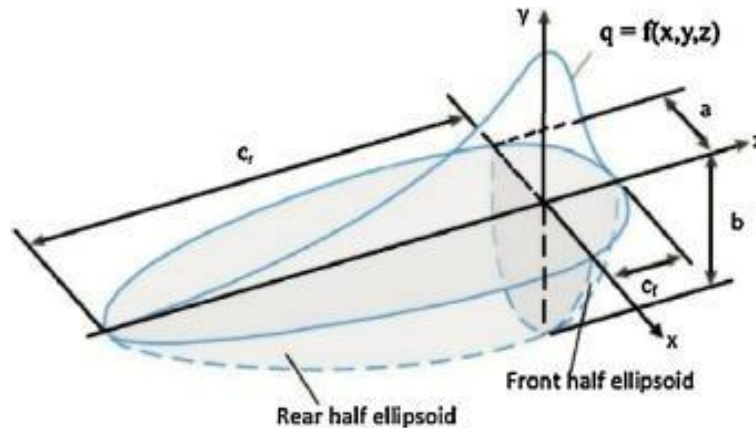


Figure 9. Goldak's double ellipsoid heat source model [16].

3. FEM Simulation on bead-on-plate

3.1 Temperature distribution

Temperature distribution of bead-on-plate process is presented in Figure 10. The temperature by previous studies suggest that the cooling time from peak temperature until 900 °C of the welding process is the most influential temperature for grain size transformation [22,23]. However, the grain size transformation has been calculated successfully by implementing a numerical model for predicting the grain size transformation for various temperature specifically.

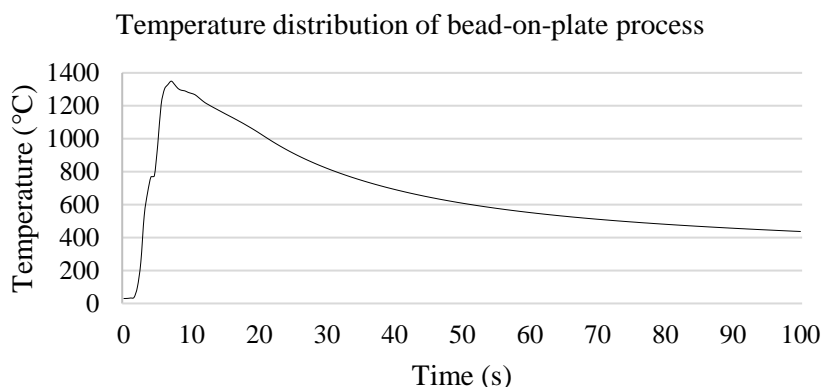


Figure 10. Temperature distribution

3.2 Grain Size

The algorithm of numerical model was developed as a preliminary study for a continuous arc welding application, where the thermal history consists of complex heating and cooling periods. Here, the temperature is transient. The numerical model can also be used for the average grain size calculations in the presence of stable alloying elements/precipitates or growing precipitates or dissolving precipitates by modifying the rate equation. The maximum average grain size depends on the peak temperature of the thermal cycle. This allow expansion and progress for more complex cases of grain size transformation. Modelling and experimental verification will focus on grain growth with growing precipitation with value of $M_0^* = 2000 \times 10^9 \text{ m}^2 \text{ s}^{-1}$.

4. Results and Discussion

Grain size prediction using the numerical model has been conducted successfully for various temperature range is shown in Table 5.

Table 5. Grain size prediction

| Initial temperature (°C) | Final temperature (°C) | Final grain size (µm) |
|--------------------------|------------------------|-----------------------|
| 1200 | Cooling temperature | 50.42 |
| 1200 | 500 | 50.21 |
| 1200 | 900 | 50.07 |
| 1300 | Cooling temperature | 50.37 |
| 1300 | 500 | 50.01 |
| 1300 | 900 | 49.89 |

5. Conclusions

The quality of any weld joint is highly influenced by the microstructure of the weldment. The layer by layer process of additive manufacturing will expose the heat affected zone (HAZ) to a complex succession of reheating cycle during the process. The progressive high temperature environment will deteriorate the quality of weldment due to metallurgical changes such as grain growth in the heat affected zone and loss of material by vaporization. Numerical simulation to predict grain size has been conducted successfully. Grain size obtained from numerical model shows good result compared to experimental results. However, by using finer mesh and greater number of increment it can be greatly improving accuracy of the simulation, but it will consume more computational time. Hence, meshing should be considered wisely. Simulation of welding process is very important not only to reduce defect of welded, but also to achieve good and expected mechanical properties. Further investigation of grain size effect towards mechanical properties of actual bead-on-plate process would give beneficial for the future studies.

Acknowledgement

The authors would like to express their gratitude to staff member of Research Interest Group: Advanced Manufacturing Technology (RIG:AMT) and Advanced Manufacturing Technology Excellence Centre (AMTEx) at Faculty of Mechanical Engineering, Universiti Teknologi MARA (UiTM) for encouraging this research. This research and conference participation are also financially supported by ASEA-UNINET grant with the project number ASEA 2019/Montan/1, ERASMUS+ (Montan University in Leoben) and Technogerma Engineering & Consulting Sdn. Bhd.

References

- [1] Lewandowski J J and Seifi M 2016 Metal Additive Manufacturing: A Review of Mechanical Properties *Annu. Rev. Mater. Res.*
- [2] Taiwade R V., Shukla R, Vashishtha H, Ingle A V. and Dayal R K 2014 Effect of Grain Size on Degree of Sensitization of Chrome-Manganese Stainless Steel *ISIJ Int.*
- [3] Chen X, Li J, Cheng X, He B, Wang H and Huang Z 2017 Microstructure and mechanical properties of the austenitic stainless steel 316L fabricated by gas metal arc additive manufacturing *Mater. Sci. Eng. A*
- [4] Mohammad Soltani H and Tayebi M 2018 Comparative study of AISI 304L to AISI 316L stainless steels joints by TIG and Nd:YAG laser welding *J. Alloys Compd.* **767** 112–21
- [5] Feng Y, Luo Z, Liu Z, Li Y, Luo Y and Huang Y 2015 Keyhole gas tungsten arc welding of AISI 316L stainless steel *Mater. Des.* **85** 24–31
- [6] Jamshidi Aval H, Serajzadeh S and Kokabi A H 2009 Prediction of grain growth behavior in haz during gas tungsten arc welding of 304 stainless steel *J. Mater. Eng. Perform.*
- [7] Saha S, Mukherjee M and Pal T K 2015 Microstructure, Texture, and Mechanical Property Analysis of Gas Metal Arc Welded AISI 304 Austenitic Stainless Steel *J. Mater. Eng. Perform.*

- [8] Kou S and Le Y 1988 Welding parameters and the grain structure of weld metal — A thermodynamic consideration *Metall. Trans. A* **19** 1075–82
- [9] DuPont J N, Lippold J C and Kiser S D 2009 *Welding Metallurgy and Weldability of Nickel-Base Alloys*
- [10] Okazaki M, Yada T and Endoh T 1989 Surface small crack growth behavior in low-cycle fatigue at elevated temperature and application limit of macroscopic crack growth law *Nucl. Eng. Des.*
- [11] Grong Ø 1997 *Metallurgical Modelling of Welding* (The Institute of Materials)
- [12] Lippold J C and Kotecki D J 2005 *Welding Metallurgy and Weldability of Stainless Steel* (Hoboken, NJ: John Wiley)
- [13] Yahya O, Manurung Y H P, Sulaiman M S and Keval P 2018 Virtual Manufacturing for Prediction of Martensite Formation and Hardness Value induced by Laser Welding Process using Subroutine Algorithm in MSC Marc / Mentat **15** 107–25
- [14] Montevecchi F, Venturini G, Scippa A and Campatelli G 2016 Finite Element Modelling of Wire-arc-additive-manufacturing Process *Procedia CIRP*
- [15] Patel L S, Patel T C, Professor A and Student M E 2014 Optimization Of Welding Parameters For TIG Welding Of 304 L Stainless Steel Using Taguchi Approach *Int. J. Eng. Dev. Res.*
- [16] Lundbäck A 2010 *Modelling and Simulation of Welding and Metal Deposition*
- [17] Ganesh K C, Vasudevan M, Balasubramanian K R, Chandrasekhar N and Vasantharaja P 2014 Thermo-mechanical analysis of TIG welding of AISI 316LN stainless steel *Mater. Manuf. Process.*
- [18] Ziętała M, Durejko T, Polański M, Kunce I, Płociński T, Zieliński W, Łazińska M, Stępniewski W, Czujko T, Kurzydłowski K J and Bojar Z 2016 The microstructure, mechanical properties and corrosion resistance of 316 L stainless steel fabricated using laser engineered net shaping *Mater. Sci. Eng. A*
- [19] Goldak J, Chakravarti A and Bibby M 1984 A new finite element model for welding heat sources *Metall. Trans. B*
- [20] Lindgren L E 2007 *Computational Welding Mechanics: Thermomechanical and Microstructural Simulations*
- [21] Hou Z B and Komanduri R 2000 General solutions for stationary/moving plane heat source problems in manufacturing and tribology *Int. J. Heat Mass Transf.* **43** 1679–98
- [22] Choi J and Mazumder J 2002 Numerical and experimental analysis for solidification and residual stress in the GMAW process for AISI 304 stainless steel *J. Mater. Sci.*
- [23] Wang Y, Ding M, Zheng Y, Liu S, Wang W and Zhang Z 2016 Finite-Element Thermal Analysis and Grain Growth Behavior of HAZ on Argon Tungsten-Arc Welding of 443 Stainless Steel *Metals (Basel)*.